Cluster Monte Carlo algorithm for the quantum rotor model

Fabien Alet[1] and Erik S. Sørensen[2]

[1]*Laboratoire de Physique Quantique and UMR 5626, Université Paul Sabatier, 31062 Toulouse, France*
[2]*Department of Physics and Astronomy, McMaster University, Hamilton, Ontario, Canada L8S 4M1*

We propose a highly efficient "worm"-like cluster Monte Carlo algorithm for the quantum rotor model in the link-current representation. We explicitly prove detailed balance for the algorithm even in the presence of disorder. For the pure quantum rotor model with $\mu = 0$, the algorithm yields high-precision estimates for the critical point $K_c = 0.333\,05(5)$ and the correlation length exponent $\nu = 0.670(3)$. For the disordered case, $\mu = \frac{1}{2} \pm \frac{1}{2}$, we find $\nu = 1.15(10)$.

What types of insulating, conducting, superconducting, and more exotic phases occur in two-dimensional systems at $T = 0$ is a topic of considerable current interest. A significant amount of theoretical [1–4] and experimental [5,6] effort has focused on bosonic systems where a superconductor to insulator transition is known to occur. In agreement with most experiments [5], it was shown under quite general conditions [1,2] that a transition can occur directly between the superconducting and insulating states. However, more recently, it has been suggested that an exotic *metallic* phase is also possible [4,6]. In this context, precise numerical results would be very valuable, and in the present paper we propose a very efficient cluster Monte Carlo algorithm for this purpose, allowing us to significantly improve previous results. In particular, we show that the inequality [7] $\nu \geq 2/d$ is *not* violated in the presence of disorder, resolving contradictions in previous work. The high precision of the algorithm should allow for precise calculations of transport properties of quantum rotor models studied theoretically in [1,4]. The ideas presented here could also be useful for the study of classical spin systems [19].

Low-dimensional bosonic systems are often described in terms of the (disordered) boson Hubbard model: $H_{bH} = \Sigma_{\mathbf{r}}[(U/2)\hat{n}_{\mathbf{r}}^2 - \mu_{\mathbf{r}}\hat{n}_{\mathbf{r}}] - t_0 \Sigma_{\langle \mathbf{r},\mathbf{r}' \rangle}(\hat{\Phi}_{\mathbf{r}}^\dagger \hat{\Phi}_{\mathbf{r}'} + \text{c.c.})$. Here U is the on-site repulsion, t_0 is the hopping strength, $\mu_{\mathbf{r}}$ is the chemical potential varying uniformly in space between $\mu \pm \Delta$, and $\hat{n}_{\mathbf{r}} = \hat{\Phi}_{\mathbf{r}}^\dagger \hat{\Phi}_{\mathbf{r}}$ is the number operator. If we set $\hat{\Phi}_{\mathbf{r}} \equiv |\hat{\Phi}_{\mathbf{r}}| e^{i\theta_{\mathbf{r}}}$ and integrate out amplitude fluctuations, H_{bH} becomes equivalent to the quantum rotor model [8]:

$$H_{qr} = \frac{U}{2} \sum_{\mathbf{r}} \left(\frac{1}{i} \frac{\partial}{\partial \theta_{\mathbf{r}}} \right)^2 + i \sum_{\mathbf{r}} \mu_{\mathbf{r}} \frac{\partial}{\partial \theta_{\mathbf{r}}} - t \sum_{\langle \mathbf{r},\mathbf{r}' \rangle} \cos(\theta_{\mathbf{r}} - \theta_{\mathbf{r}'}). \tag{1}$$

Here, $\theta_{\mathbf{r}}$ the phase of the quantum rotor, t the renormalized hopping strength, and $(1/i)(\partial/\partial\theta_{\mathbf{r}}) \simeq n_{\mathbf{r}}$. The quantum rotor model describes a wide range of phase transitions dominated by phase fluctuations, and it is well known [8] that an equivalent classical model exists where the Hamiltonian is written in terms of currents defined on the links of a lattice, $\mathbf{J} = (J^x, J^y, J^\tau)$. These link-current variables describe the "relativistic" bosonic current which should be divergence-

less, $\boldsymbol{\nabla} \cdot \mathbf{J} = 0$. In terms of these variables, the classical (2+1)D Hamiltonian can be written as follows [8]:

$$H = \frac{1}{K} \sum_{(\mathbf{r},\tau)}' \left[\frac{1}{2} \mathbf{J}_{(\mathbf{r},\tau)}^2 - \mu_{\mathbf{r}} J_{(\mathbf{r},\tau)}^\tau \right]. \tag{2}$$

Σ' denotes a summation over configurations with $\boldsymbol{\nabla} \cdot \mathbf{J} = 0$. Varying K corresponds to changing the ratio t/U in the quantum rotor model. The quantum rotor model has been extensively studied [8–10] in this representation, but a number of conclusions can be questioned due to severe finite-size effects. For notational convenience it is useful to slightly enlarge the definition of the link currents at a given site in the following way: At each site $(\mathbf{r},\tau)$ in the lattice we define *six* surrounding link variables $J_{(\mathbf{r},\tau)}^\sigma$ where σ runs over $\pm x$, $\pm y, \pm \tau$. Note that, with this notation $J_{(x,y,\tau)}^{-x}$ and $J_{(x-1,y,\tau)}^x$ is the same variable, with equivalent relations in the other directions. The divergenceless constraint at the site $(\mathbf{r},\tau)$ can then be written $J^{-x} + J^{-y} + J^{-\tau} = J^x + J^y + J^\tau$, so that the sums of the incoming and outgoing currents are equal. Conventional Monte Carlo updates [8] on this model consist of updating simultaneously four link variables. Global moves, updating a whole line of link variables thus allowing particle and winding numbers to fluctuate, are added to ensure ergodicity, but the acceptance ratio for these moves becomes exponentially small for large lattice sizes. Here we will describe a way to construct a wormlike algorithm to perform nonlocal moves for this model.

The cluster algorithm [11–13] we propose is similar in spirit to worm algorithms [14,15] in the sense that we update the link currents by moving a "worm" through the lattice visiting the sites $s_i = (\mathbf{r}_i, \tau_i)$. The links through which the worm passes are updated *during* its construction. At a given site, the links with σ equal to x, y, τ are called outgoing links and those with σ equal to $-x, -y, -\tau$ are incoming links. When the worm is moving through the lattice, the currents $J_{s_i}^\sigma$ are updated in the following manner: if the worm is leaving the site s_i along an outgoing link, we *increment* the corresponding current,

$$J_{s_i}^\sigma \to J_{s_i}'^\sigma = J_{s_i}^\sigma + 1, \quad \sigma = x, y, \tau. \tag{3}$$

If the worm is leaving the site s_i along an incoming link, we *decrement* the corresponding current,

$$J_{s_i}^\sigma \to J_{s_i}'^\sigma = J_{s_i}^\sigma - 1, \quad \sigma = -x, -y, -\tau. \tag{4}$$

The construction of the worm starts with the choice of a random initial site $s_1 = (\mathbf{r}_1, \tau_1)$ in the space-time lattice. Then the algorithm can be decomposed in two steps. (i) The worm moves to one of the six neighboring sites. To decide which direction to go from a site $s_i = (\mathbf{r}_i, \tau_i)$, we calculate for all directions $\sigma = \pm x, \pm y, \pm \tau$ weights, $A_{s_i}^\sigma$, according to local detailed balance. A good choice is

$$A_{s_i}^\sigma = \min(1, \exp(-\Delta E_{s_i}^\sigma / K)), \quad \Delta E_{s_i}^\sigma = E_{s_i}'^\sigma - E_{s_i}^\sigma. \tag{5}$$

Here $E_{s_i}^\sigma = \frac{1}{2}(J_{s_i}^\sigma)^2 - \mu_{\mathbf{r}_i} J_{s_i}^\sigma \delta_{\sigma, \pm \tau}$ is the contribution to the total energy of the link $J_{s_i}^\sigma$, before the worm moves through it. $E_{s_i}'^\sigma$ is the energy contribution with $J_{s_i}^\sigma$ replaced by $J_{s_i}'^\sigma$. By normalizing the $A_{s_i}^\sigma$'s, we define the probabilities $p_{s_i}^\sigma = A_{s_i}^\sigma / N_{s_i}$, where $N_{s_i} = \Sigma_\sigma A_{s_i}^\sigma$. A direction σ is then chosen according to these probabilities. (ii) Once σ is chosen, we update the corresponding $J_{s_i}^\sigma$ according to the above rules, Eqs. (3) and (4), and extend the worm to the new lattice site s_{i+1}. (i) and (ii) are then repeated until the worm passes through the initial site where $s_{i+1} = s_1$. Finally, in order to satisfy detailed balance, we have to *erase* the worm with a probability determined in the following way. If $N(\text{worm})$ and $N(\text{no worm})$ are the normalization of the probabilities at the initial site s_1 *with* and *without* the worm present, then we erase the constructed worm with a probability

$$P^e = 1 - \min\left(1, \frac{N(\text{no worm})}{N(\text{worm})}\right). \tag{6}$$

Under most conditions, this probability is very small. Several points are noteworthy about this algorithm. First of all, the configurations generated during the construction of the worm are not valid ($\nabla \cdot \mathbf{J} \neq 0$). However, once the construction of the worm is finished and the path of the worm closed, the divergenceless constraint is satisfied. Secondly, when the worm moves through the lattice it may pass many times through the same link and cross itself before it reaches the initial site where the construction terminates. Hence, it is crucial that the current variables are updated *during* the construction of the worm. Finally, at each step i in the construction of the worm it is likely that the worm at the site s_i will partially "erase" itself by choosing to go back to the site s_{i-1} visited immediately before, thereby "bouncing" off the site s_i.

Now we turn to the proof of detailed balance for the algorithm. Let us consider the case where the worm, w, visits the sites $\{s_1 \cdots s_N\}$, where s_1 is the initial site. The worm then goes through the corresponding link variables $\{l_1 \cdots l_N\}$, with l_i connecting s_i and s_{i+1}. Note that s_N is the last site visited before the worm reaches s_1. Hence, s_N and s_1 are connected by the link l_N. The total probability for constructing the worm w is then given by $P_w = P_{s_1}(1$
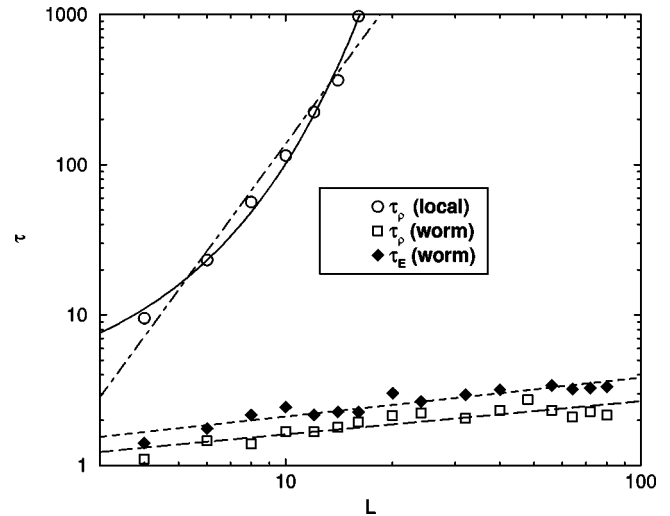

FIG. 1. Autocorrelation times versus lattice size for the conventional and worm algorithm for $\mu = 0$ at $K = 0.333$. The dashed lines indicate power-law fits and the solid line an exponential fit in L.

$-P_w^e) \Pi_{i=1}^N A_{s_i}^\sigma / N_{s_i}$. The index σ denotes the direction needed to go from s_i to s_{i+1}, P_{s_1} is the probability for choosing site s_1 as the starting point, and P_w^e is the probability for erasing the worm after construction. If the worm w has been accepted, we have to consider the probability for reversing the move. That is, we consider the probability for constructing an antiworm $\bar{w}$ annihilating the worm w. We have $P_{\bar{w}} = P_{\bar{s}_1}(1 - P_{\bar{w}}^e) \Pi_{i=1}^N \bar{A}_{\bar{s}_i}^\sigma / \bar{N}_{\bar{s}_i}$. Here, the index σ denotes the direction needed to go from $\bar{s}_i$ to $\bar{s}_{i+1}$. Note that in this case the sites are visited in the opposite order, $\bar{s}_1 = s_1, \bar{s}_2 = s_N, \ldots, \bar{s}_N = s_2$, in general $\bar{s}_i = s_{N-i+2}$ ($i \neq 1$). Note also that $\bar{s}_i$ and $\bar{s}_{i+1}$ are connected by the link $\bar{l}_i = l_{N-i+1}$, with $\bar{s}_N$ and $\bar{s}_1$ connected by $\bar{l}_N = l_1$. With this notation, we see that s_i and $\bar{s}_{N-i+1} \equiv s_{i+1}$ are connected by the link variable l_i. Let us now consider the case in which both of the worms w and $\bar{w}$ have reached the site s_i *different* from the starting site s_1. Since we are updating the link variables during the construction of the worm and since we are always considering moving the worm in all six directions, we have $N_{s_i} = \bar{N}_{\bar{s}_{N-i+2} = s_i}$ ($i \neq 1$). Furthermore, $A_{s_i}^\sigma$ and $\bar{A}_{\bar{s}_{N-i+1} = s_{i+1}}^\sigma$ only depend on the link variable l_i connecting the sites s_i and $\bar{s}_{N-i+1}$, and we see that $A_{s_i}^\sigma / \bar{A}_{\bar{s}_{N-i+1}}^\sigma = \exp(-\Delta E_{s_i}^\sigma / K)$, $i = 1 \cdots N$. Hence, since $P_{s_1} = P_{\bar{s}_1}$, we find

$$\frac{P_w}{P_{\bar{w}}} = \frac{1 - P_w^e}{1 - P_{\bar{w}}^e} \frac{\bar{N}_{\bar{s}_1}}{N_{s_1}} \exp(-\Delta E_{\text{tot}} / K), \tag{7}$$

where ΔE_{tot} is the total energy difference between a configuration with and without the worm w present. Now we consider $P^e = 1 - \min(1, N_{s_1}(\text{no worm}) / N_{s_1}(\text{worm}))$. Here, $N_{s_1} \equiv N_{s_1}(\text{no worm})$ is equal to $\bar{N}_{s_1}(\text{antiworm})$, and $\bar{N}_{s_1}(\text{no antiworm}) \equiv \bar{N}_{\bar{s}_1}$ is equal to $N_{s_1}(\text{worm})$. Hence, we find for the
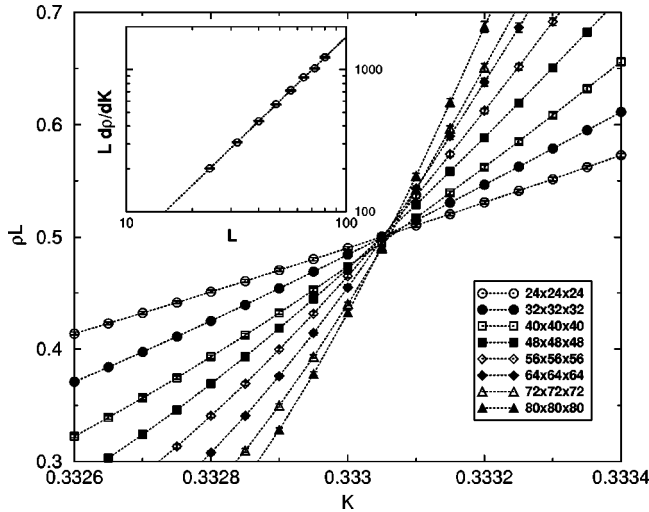
FIG. 2. $L\rho$ versus K for different lattice sizes, for $\mu=0$. All curves cross at the critical point $K_c=0.333\,05(5)$ with $L\rho|_{K=K_c}=0.495(5)$. Inset: $Ld\rho/dK$ at K_c versus L. The dashed line indicates a fit yielding an exponent $\nu=0.670(3)$.

probability to erase the worm $P_w^e=1-\min(1,N_{s_1}/\bar{N}_{s_1})$, and $P_{\bar{w}}^e=1-\min(1,\bar{N}_{s_1}/N_{s_1})$ for erasing the antiworm. With this choice of P^e, we satisfy detailed balance since $P_w/P_{\bar{w}}=\exp(-\Delta E_{tot}/K)$. Ergodicity is simply proven as the worm can perform local loops and wind around the lattice in any direction, as in the conventional algorithm.

To demonstrate the efficiency of the proposed algorithm, we have calculated autocorrelation times for different lattice sizes for the worm algorithm and the conventional algorithm. For an observable $\mathcal{O}$ we define the autocorrelation function and the autocorrelation time $\tau_\mathcal{O}$ in the usual manner [16],

$$\frac{\langle\mathcal{O}(0)\mathcal{O}(t)\rangle-\langle\mathcal{O}\rangle^2}{\langle\mathcal{O}^2\rangle-\langle\mathcal{O}\rangle^2}=ae^{-t/\tau_1}+be^{-t/\tau_\mathcal{O}}+\cdots. \quad (8)$$

Here, t is the Monte Carlo time measured in Monte Carlo sweeps (MCS), with 1 MCS corresponding to L^d attempted updates. The autocorrelation function is calculated from simulations with 10^8 MCS, and to obtain the best estimate of $\tau_\mathcal{O}$ we always fit to the indicated double-exponential form with $\tau_1\ll\tau_\mathcal{O}$. To make a fair comparison of $\tau_\mathcal{O}$ for the two algorithms, one customarily [12,16] multiplies $\tau_\mathcal{O}$ for the worm algorithm by $N/<l>$, with $<l>$ the mean number of links in a worm and $N=3L^3$. With this rescaling we show in Fig. 1 the autocorrelation times, τ_ρ for the stiffness (see the exact definition below) at $\mu=0$ for both algorithms. The calculations have been performed on cubic lattices at $K=0.333$, very near previous estimates of the critical point [9]. For the worm algorithm we also show the autocorrelation time for the energy, τ_E, which is almost identical to τ_ρ. The autocorrelation times increase dramatically with system size for the conventional algorithm, whereas they remain very small (of the order of 2–3 MCS per link) for the worm algorithm. If we fit the L dependence of $\tau_\rho\sim L^{z_{MC}}$ with a power law, we obtain an autocorrelation exponent z_{MC} larger
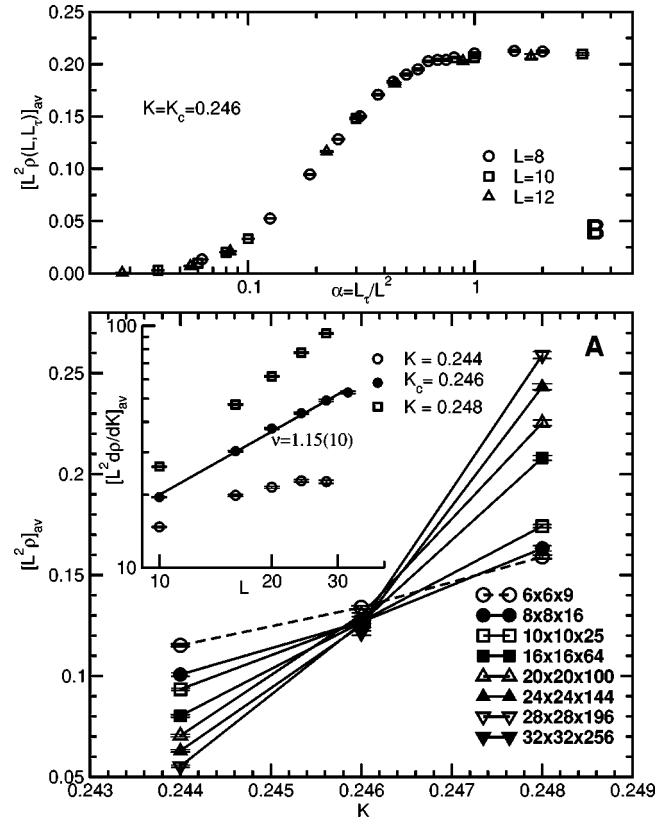

FIG. 3. (a) $[L^2\rho]_{av}$ versus K for different lattice sizes, for $\mu=\frac{1}{2}\pm\frac{1}{2}$. All curves cross at the critical point $K_c=0.246(1)$ with $[L^2\rho]_{av}|_{K=K_c}=0.12(1)$. Inset: $[L^2d\rho/dK]_{av}$ versus L for different K. The solid line indicates a power-law fit yielding an exponent $\nu=1.15(10)$. (b) Scaling plot of $L^2\rho(L,L_\tau)$ at $K_c=0.246$.

than 4 for the conventional algorithm. For the conventional algorithm, it is likely that τ_ρ is diverging exponentially with L since ρ is solely determined by global updates for which the acceptance probability decreases exponentially with L. For the worm algorithm, we find a very small $z_{MC}\sim0.3$.

We now present results for the model Eq. (2) at $\mu=0$. There, the model is expected to undergo a transition in the $(2+1)$D XY universality class [1,9] from a superfluid into a Mott insulating phase with a dynamical critical exponent $z=1$. The different phases can be distinguished by calculating the stiffness defined as [8]

$$\rho=\frac{1}{L_\tau L^2}\left\langle\left(\sum_{\mathbf{r},\tau}J_{(\mathbf{r},\tau)}^x\right)^2\right\rangle. \quad (9)$$

Since we expect $z=1$, we use L_τ, the system size in the third direction, equal to L. To obtain the K dependence of ρ, we have used reweighting techniques [17] on large runs (of the order of 10^8 MCS) at $K=0.333$. The error bars are determined using jackknife techniques [16]. Using finite-size scaling relations, the quantity ρL^z is expected to be independent of system size at the critical point [8], K_c. Moreover, $L^z d\rho/dK$ is expected to diverge at K_c as $L^{1/\nu}$ where ν is the correlation length exponent. We have explicitly calculated this quantity by evaluating the thermodynamic derivative of

ρ with respect to the coupling K: $d\rho/dK=(\langle\rho E\rangle-\langle\rho\rangle\times\langle E\rangle)/K^2$. In Fig. 2, we show $L\rho$ versus K for different lattice sizes. From the crossing of the curves we can determine $K_c=0.333\,05(5)$ to a much higher precision than was possible using the conventional algorithm on much smaller systems [8–10]. Since all the curves cross in a single point, our results are completely consistent with a dynamical exponent $z=1$, as expected [1]. In the inset of Fig. 2 is shown the size dependence of $L^z d\rho/dK$ at K_c on a log-log scale. We fit this curve to a power-law $AL^{1/\nu}$ and obtain $\nu=0.670(3)$, in perfect agreement with estimates for the three-dimensional XY universality class [18]. Preliminary results [19] for the *generic* transition at $\mu=\frac{1}{4}$ show pronounced finite-size effects questioning previous work [10].

We also simulated the model Eq. (2) with disorder for $\mu=\frac{1}{2}\pm\frac{1}{2}$. In this case, the transition is between a superfluid and an insulating Bose-glass phase. Scaling theory [1] predicts a second-order transition with dynamical exponent $z=2$. Hence, we use lattices of size $L\times L\times \alpha L^2$, where $\alpha=L_\tau/L^2$ is the aspect ratio. Previous work [8], limited to $L\leq10$, has determined $K_c=0.248\pm0.002$. Estimates for the correlation length exponent [8,10] yielded $\nu=0.9\pm0.1$, almost violating the inequality [7] $\nu\geq2/d$. From the results shown in Fig. 3(a), obtained with the cluster algorithm, it is clear that K_c is in fact at a slightly lower value K_c $=0.246(1)$, although the crossing of $L=6,8$ occurs at $K=0.248$. The disorder average, $[\cdot]_{\mathrm{av}}$, has been performed over 50 000 samples with 10^5 MCS per sample. The more precise value for K_c significantly changes estimates of ν. The inset in Fig. 3(a) shows $[L^2 d\rho/dK]_{\mathrm{av}}$ versus L, which at K_c yields $\nu=1.15(10)$, now largely satisfying the inequality $\nu\geq2/d$. The results in Fig. 3(a) are clearly consistent with $z=2$. In Fig. 3(b) we show results for $L^2\rho(L,L_\tau)$ versus L_τ/L^2 at K_c. Standard scaling theory [20] predicts that this should be a universal function of α if $z=2$. Our results confirm this nicely. The values of exponents are in good agreement with the analytical estimates in [21].

In conclusion, we have introduced a worm algorithm for the quantum rotor model. For the link-current representation of the quantum rotor model, the proposed algorithm is exponentially more efficient than conventional algorithms and performs at par with the Wolff algorithm [12] for the classical 3D XY model. Most noteworthy, the algorithm performs exceptionally well on disordered systems. We have also successfully adapted it to the study of systems with longer-range interactions as well as classical Ising models [19].

[1] See M. P. A. Fisher, P. B. Weichman, G. Grinstein, and D. S. Fisher, Phys. Rev. B **40**, 546 (1989), and references therein.

[2] M. P. A. Fisher, G. Grinstein, and S. M. Girvin, Phys. Rev. Lett. **64**, 587 (1990).

[3] K. Damle and S. Sachdev, Phys. Rev. B **56**, 8714 (1997).

[4] D. Das and S. Doniach, Phys. Rev. B **60**, 1261 (1999); P. Phillips and D. Dalidovich, *ibid.* **65**, 081101 (2002); D. Dalidovich and P. Phillips, Phys. Rev. Lett. **89**, 027001 (2002); A. Paramekanti, L. Balents, and M. P. A. Fisher, Phys. Rev. B **66**, 054526 (2002).

[5] See Y. Liu and A. M. Goldman, Physica D **83**, 163 (1995), and references therein.

[6] See N. Mason and A. Kapitulnik, Phys. Rev. Lett. **82**, 5341 (1999), and references therein.

[7] J. T. Chayes *et al.*, Phys. Rev. Lett. **57**, 2999 (1986).

[8] E. S. Sørensen *et al.*, Phys. Rev. Lett. **69**, 828 (1992); M. Wallin *et al.*, Phys. Rev. B **49**, 12 115 (1994).

[9] M.-C. Cha *et al.*, Phys. Rev. B **44**, 6883 (1991).

[10] A. v. Otterlo and K.-H. Wagenblast, Phys. Rev. Lett. **72**, 3598 (1994); A. v. Otterlo *et al.*, Phys. Rev. B **52**, 16 176 (1995); J. Kisker and H. Rieger, *ibid.* **55**, R11981 (1997), Physica A **246**, 348 (1997); S. Y. Park *et al.*, Phys. Rev. B **59**, 8420 (1999); J.-W. Lee, M.-C. Cha, and D. Kim, Phys. Rev. Lett. **87**, 247006 (2001).

[11] R. H. Swendsen and J. S. Wang, Phys. Rev. Lett. **58**, 86 (1987).

[12] U. Wolff, Phys. Rev. Lett. **62**, 361 (1989).

[13] H. G. Evertz, G. Lana, and M. Marcu, Phys. Rev. Lett. **70**, 875 (1993).

[14] N. V. Prokof'ev, B. V. Svistunov, and I. S. Tupitsyn, Phys. Lett. A **238**, 253 (1998); N. V. Prokof'ev and B. V. Svistunov, Phys. Rev. Lett. **87**, 160601 (2001).

[15] A. W. Sandvik, Phys. Rev. B **59**, R14157 (1999).

[16] M. E. J. Newman and G. T. Barkema, *Monte Carlo Methods in Statistical Physics* (Oxford University Press, Oxford, 1999).

[17] A. M. Ferrenberg and R. H. Swendsen, Phys. Rev. Lett. **61**, 2635 (1988).

[18] M. Campostrini *et al.*, Phys. Rev. B **63**, 214503 (2001).

[19] F. Alet, P. Hitchcock, and E. S. Sørensen (unpublished).

[20] M. Guo, R. N. Bhatt, and D. A. Huse, Phys. Rev. Lett. **72**, 4137 (1994); H. Rieger and A. P. Young, *ibid.* **72**, 4141 (1994).

[21] I. F. Herbut, Phys. Rev. B **57**, 13729 (1998).